Layout: T3_Grey Book ID: 454584_1_En Book ISBN: 978-3-030-10373-6
Chapter No.: 5 Date: 4-3-2019 Time: 2:23 pm Page: 61/75

5 An Integrated Machine Learning Approach for Automatic Highway Extraction from Airborne LiDAR Data and Orthophotos

5.1 Introduction

Automatic extraction of highways from airborne LiDAR (light detection and ranging) has been a long-standing active research topic in remote sensing. Accurate and computationally useful extraction of highway information from remote sensing data is significant for various applications such as traffic accident modeling (Bentaleb et al. 2014), navigation (Kim et al. 2006), intelligent transportation systems (Vaa et al. 2007), and natural hazard assessments (Jebur et al. 2014). Although there have been many studies on extracting road networks from satellite images, the information extracted from those images is limited to two-dimensional information and accurate 3D geometry hard to get. The recent advances in LiDAR technology permit accurate scanning of earth surface and ground objects (i.e., roads and buildings) in both two and three dimensions. In other words, LiDAR provides accurate and high-resolution horizontal and vertical spatial points (Antonarakis et al. 2008). Furthermore, LiDAR technology allows for acquiring both spatial (three-dimensional locations) and spectral (intensity values) information about earth surface and ground objects (Antonarakis et al. 2008). The acquired data represent height surfaces that include artificial and natural objects. On the other hand, the intensity is defined as a ratio of signal strength at transmission to signal strength at detection (Alharthy and Bethel 2003). Concerning these advances and high-resolution laser scanning data, the task of road extraction is usually approached by two main steps: road detection and vectorization (White et al. 2010). The process of road detection is to separate road point clouds from other objects, while vectorization process is the extraction of detailed road polygons. Roads usually have relatively constant height compared to building or other structures in urban areas, and the elevation shows gradual changes in slope for safety reasons (Choi et al. 2008). These characteristics can be used to distinguish roads from other features. However, for accurate road extraction, information derived from LiDAR data is not enough due to the complexity of separation of roads from other ground points with the similar intensity value (Gong et al. 2010). In addition, LiDAR intensity values are affected by several factors such as surface reflectance, transmitted power, atmospheric attenuation, and incidence angle and range distance (Coren and Sterzai 2006). Apart from that, roads have missing data due to above obstacles (e.g., trees and vehicles), noise data (e.g., road markings), and different types of materials (e.g., asphalt and concrete). Therefore, incorporating color information from aerial photos is critical for accurate road extraction (Gong et al. 2010).

Machine learning (ML) is a subfield of computer science and artificial intelligence based on the biological learning process. ML explores the study, design, and construction of algorithms to learn from the past and make predictions on a new set of data (Lary et al. 2015). ML covers main areas such as data mining, statistics, and software applications. It is a collection of a variety of algorithms (e.g., neural networks, support vector machines, self-organizing map, decision trees, logistic regressions, genetic programming, etc.). ML is an efficient empirical method for both regression and classification of nonlinear systems (Lary et al. 2015). Several methods based on ML were proposed for remote sensing applications and mostly for image classification (Butenuth et al. 2003; Song and Civco 2004; Bazi and Melgani 2006). Specifically, neural networks (NN) have been applied to remote sensing image classification. Despite its success in this area, a significant limitation of this model is the fact that their computational complexity is quite high (Ding et al. 2013) and it has a drawback of overlearning (Baczyński and Parol 2004). Additionally, support vector machine (SVM)-based approaches have also been extensively used for image classification (Bazi and Melgani 2006). The reason behind SVM's popularity in this area is its capability to produce higher classification accuracy than the NN model (Bazi and Melgani 2006). However, the choice of the suitable kernel function, kernel specific parameters, and regularization parameter is some of the major concerns in the design of an SVM model (Mountrakis et al. 2011). Apart from the

B. Pradhan and M. Ibrahim Sameen, *Laser Scanning Systems in Highway and Safety Assessment*, Advances in Science, Technology & Innovation,
https://doi.org/10.1007/978-3-030-10374-3_5

methods above, logistic regression and decision tree algorithms were extensively used for remote sensing image analysis as well (Friedl and Brodley 1997).

5.2 Previous Related Works

Several methods have been proposed in the literature for road detection from high-resolution satellite images and aerial photographs. The common used approaches include region growing (Amo et al. 2006; Mena and Malpica 2005), segmentation and clustering (Wan et al. 2007), machine learning (Butenuth et al. 2003; Song and Civco 2004), and snake models (Song and Civco 2004; Peng et al. 2010). However, due to the complexity of the recent highway designs, road detection from aerial images is a challenge. Besides, aerial images are easily influenced by occlusion, shadow, spectrum similarity of different objects, and heterogeneous spectra (Rottensteiner 2009; Zhao and You 2012). In addition, information extracted from satellite images is limited to 2D, and complete road geometry is difficult to be extracted. Therefore, a fusion of LiDAR data with aerial images has become an essential phenomenon, which overcomes the shortcomings above of aerial images (Zhu et al. 2009; Clode et al. 2004; Hu et al. 2004). By using LiDAR data, the known elevations can be used to efficiently discriminate between roads and other aboveground objects with same spectra such as buildings (Poullis and You 2010; Rottensteiner 2010). On the other hand, LiDAR intensity and aerial images allow distinguishing roads from other bare land and grasslands, which have similar elevation (Gong et al. 2010).

In addition to the methods proposed above for extracting roads from aerial images, several approaches have been developed to extract roads from LiDAR data. In a recent paper, (Zhu et al. 2004) presented an automatic road extraction technique that combines information from aerial photographs and laser scanning data. The method utilized road edges shadowed by surrounding high objects, such as tall buildings and trees. This method is difficult to implement in conventional GIS software. In addition, the method is limited to the roads where the tall objects are present, which is not the case always. An automatic method based on morphological filtering of intensity image was proposed by Clode et al. (2004). Object-based image analysis approach was used for road extraction from LiDAR data by several authors (Brennan and Webster 2006; Hodgson et al. 2008; Zhou 2013). Although object-based approach is proven an efficient way for feature extraction, however, it is very challenging to develop transferable rulesets in this approach. Furthermore, a parallel algorithm for the extraction of road point clouds was proposed for LiDAR data by Li et al. (2008) using intensity and height information. There are still noisy points over the road, and in some cases, points were missing in narrow places such as parking lots and residential sub-district. The roads of these areas are wider than normal road; however, they may use the same material as a road. In order to handle these kinds of problems, the more complicated algorithms are required. Reference (Samadzadegan and Bigdeli 2009) used multiple classifier system to extract roads from LiDAR point clouds. A *k*-means clustering method based on intensity data was used to extract roads from LiDAR data by Gong et al. (2010), and the result was refined by using the spectrum information of aerial images. Moreover, (Zhao et al. 2011) described an unsupervised approach for efficient extraction of grid-structured urban roads from airborne LiDAR data. A mean shift algorithm was used by Wang et al. (2011) for road extraction from LiDAR data. In this method, both LiDAR and aerial photographs were fused and the color space of aerial photograph was transformed into L-a-b color space system. Compared with other traditional classification methods, the mean shift algorithm is more suitable in multidimensional data classification. However, when there are two or more features spectrally similar, the algorithm produces low-quality results. Reference (Zhao and You 2012) proposed an original procedure for road extraction from aerial LiDAR data. The procedure combines a robust local detector with a global context-incorporating graph to reach both high correctness and completeness. More recently, (Hu et al. 2014) proposed to use multiple features to detect road centerlines from the remaining ground points after filtering. The main idea of the method was to detect smooth geometric primitives of potential road centerlines and to separate the connected non-road features (parking lots and bare grounds) from the roads. One problem with this approach is the heavy computational cost in the tensor-voting step. Another problem is the recognition of the contextual objects of roads, such as lane markings, road junction patterns, vehicles, and road edges.

Although previous researchers have made many efforts, the problem of automatic road detection is still far from being solved (Zhu et al. 2009; Clode et al. 2004; Boyko and Funkhouser 2011). Therefore, this study aims to evaluate several ML algorithms (i.e., multilayer perceptron, support vector machine, logistic regression, and decision trees) for extracting roads from airborne LiDAR integrated with aerial orthophotos. To build an integrated model for automatic road extraction from LiDAR data, this study proposed an efficient integrated GIS workflow. The main contribution of this study is analyzing several machine learning algorithms and testing their transferability for road extraction from LiDAR data. In addition, the study developed an integrated GIS model based on the best machine learning algorithm identified. The integrated model proposed here differs to those presented above is that it is transferable and straightforward which means the model could be applied to different AQ1

LiDAR datasets. This paper presents first a brief literature review about automatic road extraction from LiDAR data and then gives a theoretical background on the used machine learning algorithms (multilayer perceptron neural networks, support vector machine, logistic regression, and decision trees). After that, a systematic methodology was presented. Finally, the results obtained from the proposed GIS workflow were presented and discussed.

5.3 Machine Learning Models

In this study, several machine learning algorithms were evaluated for road detection from airborne LiDAR data and aerial photographs. The algorithms used in this study are multilayer perceptron neural networks, support vector machine, logistic regression, and decision tree. These methods have been commonly used for remote sensing data analysis and information extraction. However, there were not many studies investigated these methods for automatic road extraction, and comprehensive comparison study was not done among them. The following sections present the concept and background information on these algorithms.

5.3.1 Multilayer Perceptron Neural Networks (MLP)

In machine learning, neural networks are a family of statistical, biological learning models. Multilayer perceptron consists of a system of simple interconnected neurons or nodes, as illustrated in Fig. 5.1. It is a model representing a nonlinear mapping between some inputs and outputs. Neurons are usually organized into layers with full or random connections between successive layers (Mokhtarzade and Zoej 2007). Conceptually, there are three types of layers: input, hidden, and output layers that receive process and present the results, respectively (Mokhtarzade and Zoej 2007). The nodes are connected by numeric weights and output signals, which are a function of the sum of the inputs to the node modified by a simple activation function (Gardner and Dorling 1998).

What has attracted the research fraternity the most in neural networks is the possibility of learning. The most common learning algorithm for neural networks is the backpropagation, which was developed by Paul Werbos in 1974 and rediscovered independently by Rumelhart and Parker (Priddy and Keller 2005). It is an iterative gradient algorithm designed to minimize the error function (Eq. 5.1). Despite the success of such neural networks in remote sensing applications, a significant limitation of this model is the fact that their computational complexity is quite high and it has a drawback of overlearning (Baczyński and Parol 2004; Mia et al. 2015).

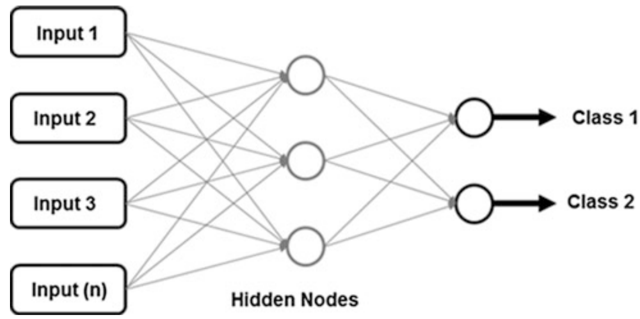

Fig. 5.1 A simple structure of multilayer perceptron neural network

$$E = \frac{1}{2}\sum_{i=1}^{L}\left(d_j - o_j^M\right)^2 \tag{5.1}$$

where d_j and o_j^M represent the desired output and current response of the node 'j' in the output layer, respectively, and 'L' is the number of nodes in the output layer. In an iterative method, corrections to weight parameters are computed and added to the previous values as illustrated in Eq. (5.2):

$$\begin{cases} \Delta w_{i,j} = -\mu \dfrac{\partial E}{\partial w_{i,j}} \\ \Delta w_{i,j}(t+1) = \Delta w_{i,j} + \alpha \Delta w_{i,j}(t) \end{cases} \tag{5.2}$$

where $w_{i,j}$ is weight parameter between node i and j, Δ a positive constant that controls the amount of adjustment and is called learning rate, α a momentum factor that can take on values between 0 and 1 and 't' denotes the iteration number. The parameter α can be called smoothing or stabilizing factor as it smoothest the rapid changes between the weights (Yang 1995). AQ2

5.3.2 Support Vector Machine (SVM)

Support vector machine (SVM) is a statistical classification method proposed by Vapnik (2013). Given m labeled training samples, $\{(\vec{x}_i, \vec{y}_i | \vec{x}_i \in R^n, y_i \in \{-1, 1\}, i = 1\ldots m,$ SVM is able to generate a separation hypersurface that has maximum generalization ability. Mathematically, the decision function can be formulated as represented in Eq. (5.3).

$$\mathrm{d}(\vec{x}) = \sum_{i=1}^{m} \alpha_i y_i K(\vec{x}_i, \vec{x}) + b \tag{5.3}$$

where α_i and b are the parameters determined by SVM learning algorithm, and $K\left(\vec{x}_i, \vec{x}\right)$ is the kernel function (refer to Table 5.1 for common kernel functions used with SVM) which implicitly maps the samples to a higher dimensional space. Those samples $\vec{x}_i$ with nonzero parameters α_i are called 'support vectors' (SVs). The accuracy with which an SVM can classify a dataset depends on the magnitude of the parameter C (Matkan et al. 2014), where C is a penalty term that controls the magnitude of penalty associated with the training samples classified on the wrong side of the hyperplane (Oommen et al. 2008). Details of SVM can be found in Matkan et al. (2014); Melgani and Bruzzone (2004); Zhan and Shen (2005).

As with any machine learning technique, SVM needs to learning algorithm to get experience from training data and make predictions on data. The common learning technique used with SVM is quadratic programming (QP) (Platt 1999). However, this algorithm is expensive in computational costs (Platt 1999). Sequential minimal optimization (SMO) is a simple algorithm that quickly solves the SVM quadratic programming (QP) problem without an iterative numerical routine for each sub-problem (Platt 1999). SMO decomposes the overall QP problem into QP sub-problems similar to Osuna's method (Melgani and Bruzzone 2004). SMO chooses to solve the smallest possible optimization problem at every step. For the standard SVM QP problem, the smallest possible optimization problem involves two Lagrange multipliers because the Lagrange multipliers must obey a linear equality constraint. At every step, SMO chooses two Lagrange multipliers to optimize, finds the optimal values for these multipliers, and updates the SVM to reflect the new optimal values.

5.3.3 Logistic Regression (LR)

The logistic regression (LR) is an efficient mathematical model used Logistic regression (Logit) analysis has also been used to investigate the relationship between binary or ordinal response probability and explanatory variables (Nandi and Shakoor 2010). This model is represented by a linear equation as described by Jebur et al. (2014) as following:

$$Y = b_0 + b_1 x_1 + b_2 x_2 + \cdots + b_n x_n \quad (5.4)$$

where Y shows the dependent layer, it could be (1) or (0), b_0 is the intercept of the model, $b_i = (i = 0, 1, 2, \ldots, n), b_i (i = 0, 2, \ldots, n)$ represents the LR coefficients, and $x_i (i = 0, 1, 2, \ldots, n)$ denotes the causative factors.

To make predictions on the possibility of an event in each pixel, the probability index can be measured by using Eq. (5.5).

$$p = \frac{1}{1 + e^{-Y}} \quad (5.5)$$

where p is the target probability attained between 0 and 1 on an S-shaped curve.

5.3.4 Decision Tree (DT)

A decision tree is a treelike model and supervised classifier designed to classify input training data into more homogenous subgroups using constructed rules or decisions called nodes (Friedl and Brodley 1997; Quinlan 2014). DT is commonly used in machine learning, statistics, and data mining to create a model that predicts the value of a target variable based on several input variables. During the training process, DT aims to obtain maximum information and minimum entropy in the generated model (Quinlan 2014). The decision tree consists typically of nodes, which stand for circles, and the branches stand for segments connecting the leaf nodes. DT can be implemented in WEKA (Waikato Environment for Knowledge Analysis) open-source software under the tree function called J48. J48 is slightly modified C4.5 (Gokgoz and Subasi 2015) in which generates a classification–decision tree for the given dataset by recursive partitioning of data (Zhao and Zhang 2008). The algorithm takes into account of all the possible tests that can split the dataset and selects a test that gives the best information gain. AQ3 It passes through the decision tree, visits each node, and selects optimal subset (Mašetic and Subasi 2013). It is achieved by using the gain ratio, represented by Eqs. (5.6) and (5.7):

$$\text{Gain Ratio}(S, A) = \frac{\text{Information Gain }(S, A)}{\text{Entropy }(S, A)} \quad (5.6)$$

$$\text{Entropy}(S) = -p_{\text{p}} \log_2 p_{\text{p}} - p_{\text{n}} \log_2 p_{\text{n}} \quad (5.7)$$

Table 5.1 Kernel functions used with SVM classification. *Source* Yao and Han (2011); Soliman and Mahmoud (2012)

Function type	Equation
Linear kernel function	$K(x_i, x_j) = x_i^T x_j$
Polynomial kernel function	$K(x_i, x_j) = (\gamma x_i^T x_j + r)^d, \quad \gamma > 0$
Radial basis function	$K(x_i, x_j) = e^{(-\gamma x_i - x_j^2)}, \quad \gamma > 0$
Sigmoid kernel function	$K(x_i, x_j) = \tanh(\gamma x_i^T x_j + r)$

where S is a training set, A is an attribute, p_p is the proportion of positive examples in S, and p_n is the proportion of negative examples in S (Saghebian et al. 2013).

5.4 Study Area

The study area is a subset corridor from the longest expressway in Malaysia (North–South Expressway [NSE]), running from Bukit Kayu Hitam in Kedah near the Malaysian–Thai border to Johor Bahru at the southern portion of Peninsular Malaysia (Fig. 5.2). This subset was selected because the highway located in this area is surrounded by various bare earth types (i.e., bare soil, low vegetation, construction site), which is important to take into consideration for highway extraction.

5.5 Data and Methodology

The LiDAR data used in this study were collected on March 8, 2013, by Riegl LM Q5600 and Camera Hassleblad 39 Mp. The device has a spatial resolution of 13 cm, laser scanning angle of 60°, and camera angle of 45°. In addition, the posting density of the LiDAR data was 3–4 pts/m^2.

In this study, it was assumed that road extraction from LiDAR data is a two-class classification problem (roads and non-roads classes). Using variables derived from LiDAR data and aerial photographs (i.e., height, intensity, color) together with machine learning techniques, various models can be developed to optimize the separation of the two classes. Thus, roads can be extracted by applying a simple threshold value. Because there are several artificial and natural features have similar characteristics with roads such as bare earth (similar height) and concrete roads (similar intensity), the color information extracted from aerial photographs combining with variables derived from LiDAR can be useful for developing generalized models for road extraction.

5.5.1 Data Preprocessing

5.5.1.1 Generation of Digital Elevation Model (DEM)

The raw LiDAR data include three-dimensional coordinates of ground points and surface points. Those two sets of data can be used to generate DEM and digital surface model (DSM) in grid form (Briese et al. 2002). In this study, the raw LiDAR point clouds, first, were filtered based on the last pulse return and then a DSM was generated using the nearest neighbor interpolation technique in ArcMap 10.3 software (Fig. 5.3a). Next, the multiscale curvature classification (MCC) algorithm was used in the same software to remove the non-ground points (Fig. 5.3b). MCC is an iterative multiscale algorithm for classifying LiDAR returns as ground and non-ground (Evans and Hudak 2007). The MCC algorithm was developed at the Moscow Forestry Sciences Laboratory of the USFS Rocky Mountain Research Station. In short, the algorithm integrates curvature filtering with a scale component and variable curvature tolerance. During this stage, a surface was interpolated at different resolutions using the thin-plate spline method (Evans and Hudak 2007) and points were classified based on a progressive curvature threshold parameter; the curvature tolerance parameter increases as resolution coarsens to compensate for slope effect as the data are generalized. Figure 5.3b shows the DEM generated using MCC algorithm in ArcMap 10.3 software.

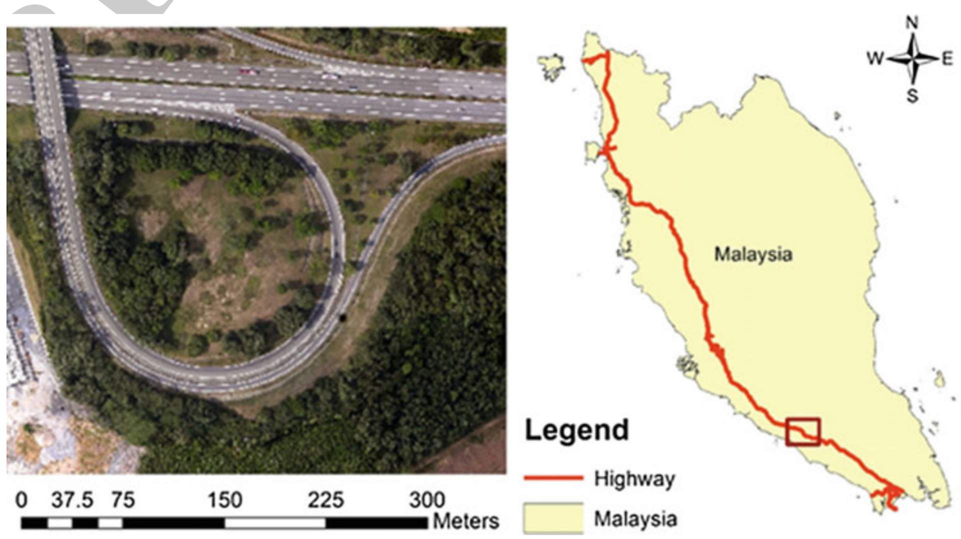

Fig. 5.2 Location of the study area

Layout: T3_Grey Book ID: 454584_1_En Book ISBN: 978-3-030-10373-6
Chapter No.: 5 Date: 4-3-2019 Time: 2:23 pm Page: 66/75

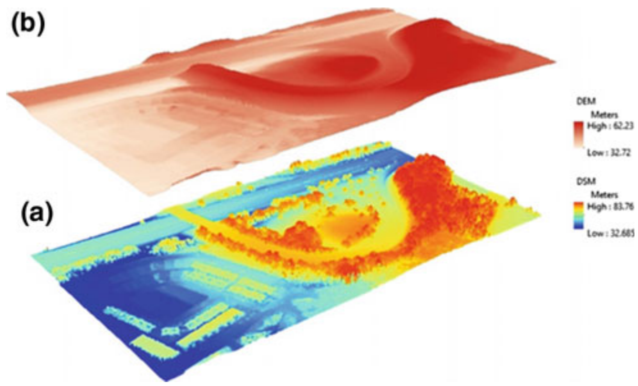

Fig. 5.3 Products derived from the raw LiDAR data, **a** DSM, **b** DEM

5.5.1.2 Color Space Transformation

One of the challenges in developing generalized models for image classification and feature extraction is the non-systematic effects on the spectral signature such as illumination effects (Wang et al. 2011). There are several color space models which have been developed to represent the color as tuples of numbers such as RGB and L-a-b color models (Wang et al. 2011). The space L-a-b was especially designed to best approximate human vision. In both cases, L, the lightness (relative brightness) coordinate, is defined in the same way; the two spaces differ only through the chromaticity coordinates (Wang et al. 2011). The L-a-b color space includes all perceivable colors, which means that its gamut exceeds those of the RGB color model. Thus in this study, we converted the RGB aerial photographs into the L-a-b color model to reduce the illumination effects from the original images.

5.5.2 Preparation of Input Attributes and Training/Testing Samples

Based on the assumptions discussed above, four attributes (i.e., height [nDSM], NDIR, intensity, color) were used as inputs for the models. To prepare these variables for the model development purposes, the related products from LiDAR and digital orthophoto data were subsequently generated. The height raster (nDSM) was generated by subtracting the DEM from DEM layer (Fig. 5.4d). LiDAR data usually come with the intensity attribute linked to the point clouds. Thus, these attributes were used to generate the intensity raster by interpolating the points using nearest neighbor method (Fig. 5.4a). The intensity layer was smoothened using a simple mean filter with (3 × 3) window size. On the other hand, the color raster was generated from the digital orthophoto by using band rationing for the b^* and a^* bands extracted from the transformed orthophoto (Fig. 5.4b). In addition, to these layers, one more layer was used is the intensity raster and the b^* band of color raster where combined to produce additional attribute to investigate its contribution to the highway extraction (Fig. 5.4c). The formula used for the combination of intensity and b^* band raster is represented by Eq. (5.8), and the result of this calculation was named normalized difference intensity and red (NDIR) index. AQ4

$$\mathrm{NDIR} = \frac{\mathrm{Intensity} - b^*}{\mathrm{Intensity} + b^*} \tag{5.8}$$

Ground reference data for the study area were generated based on random sampling procedure from the preprocessed data. First, the highway features were digitized manually to create the vector format of the raster data. Using the random point generator tool in ArcMap 10.3 software, a total number of 1700 points were generated randomly with a constraint that the minimum distance between each point is not less than 1 m. These generated points were distributed for both classes (highway and others). As a result, each class had the same number of points located within the class polygons and was equal to 850 points for each. Next, the attributes (height, NDIR, intensity, and color) were extracted from the corresponding raster and linked to the point feature class. Then, the attributes of the point feature class were exported to Microsoft Excel software and organized in such a way that is readable in Weka 3.6.0 software. The 850 sampling points were then divided into two equal groups for training (50%) and testing (50%), and those used for models development.

5.5.3 Proposed GIS Workflow for Automatic Highway Extraction

The method proceeded by taking the raw LiDAR data and produced both DSM and DEM using the method explained before. In addition, it takes the intensity attributes stored in the raw point clouds and generates intensity raster by using the nearest neighbor interpolation. In parallel, it takes the aerial photograph in RGB format and converts it to L-a-b format. Then, using the L-a-b image and LiDAR intensity, it creates a new raster data (NDIR) using the band ratio procedure (explained in Sect. 5.2). After that, it prepares the generated set of raster datasets as inputs for the proposed models to detect the highway features in the image scene. Using the proposed models and generated inputs, the initial highway layer can be produced. Because the initial result from the highway detection models has noises, the post-processing is then applied. In the post-processing stage, a majority filter was applied to reduce the noises and at the same time fills the gaps between the points. In short, a majority filter assigns every pixel to the majority category within an $n \times n$ window surrounding the pixel. In this study,

Layout: T3_Grey Book ID: 454584_1_En Book ISBN: 978-3-030-10373-6
Chapter No.: 5 Date: 4-3-2019 Time: 2:23 pm Page: 67/75

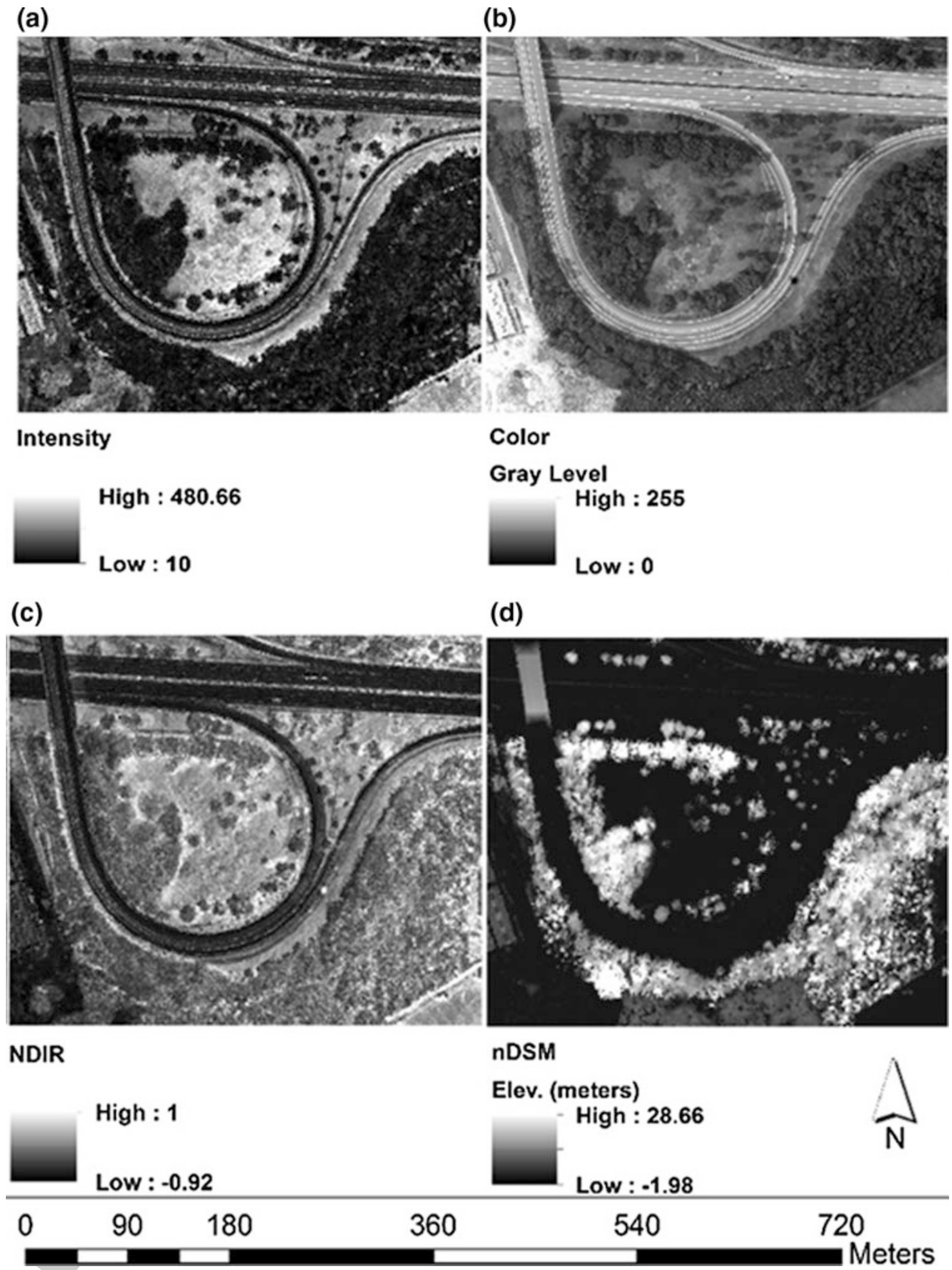

Fig. 5.4 Input raster produced from LiDAR and digital orthophoto data, **a** intensity raster, **b** color raster, **c** NDIR raster, **d** height (nDSM) raster

a window size of 5 × 5 was used to balance between removing the noises and resolving the boundary of the features. Finally, the refined product of highway raster is produced for various purposes.

5.6 Results and Discussion

For auditing the results of the proposed models and GIS workflow, we assessed the developed ML models in general and discussed the factors affecting the accuracy of the results of the models. After that, the quality of the proposed GIS workflow was evaluated by an application on a raster data using an accuracy assessment strategy introduced by Wiedemann et al. (1998), which is based on three indices, i.e., completeness, correctness, and quality measures. The ground reference highway was digitized manually based on the aerial photograph using polygon feature class, producing high-quality reference data with complete details of roads presented in the study area. The subsequent sections discuss the results obtained and the evaluation process for each model and the simple integrated GIS workflow.

Layout: T3_Grey Book ID: 454584_1_En Book ISBN: 978-3-030-10373-6
Chapter No.: 5 Date: 4-3-2019 Time: 2:23 pm Page: 68/75

5.6.1 Proposed Models for Highway Extraction

In this study, we applied four machine learning-based models for highway extraction from airborne LiDAR data integrated with aerial orthophotos. First, the four attributes derived from LiDAR and aerial photograph data at each sampling points were used to build a multilayer perceptron neural network model. During the model development process, the effect of several factors was investigated which might affect the classification accuracy such as a number of hidden nodes and layers as well as to the learning rate and momentum parameters. These issues were discussed in the next sections.

A new linear model was developed for highway extraction based on SVM approach. This model is shown in Table 5.2, which is a simple model by taking into consideration of four inputs and produces an output that could be the threshold to detect the highway features in the data. The overall accuracy of (90.19%) with the best *C* parameter used polynomial kernel function was achieved. *C* values and other kernel function types were investigated in more details, which are discussed in the next sections.

Additionally, a logistic regression model was also developed. The logistic regression model permits extracting roads from LiDAR and aerial photograph data with an elementary mathematical model and threshold value with no user-defined parameters. The logistic regression model developed in this study is shown in Table 5.2. Furthermore, a decision tree (DT) algorithm was also utilized to develop a model for highway extraction from the same data. In the DT model, collections of linear rules were developed to classify the input parameters into two binary classes (roads and non-roads). The complete DT algorithm is presented in a graphical form in Fig. 5.5.

5.6.2 Accuracy Assessment

The overall accuracy assessment of the proposed models (Fig. 5.6) was based on three measures: overall accuracy, Kappa coefficient, and user accuracy of highway class. In addition, during this evaluation process, the best user-defined parameters were used for each model. This evaluation showed that MLP model achieved the highest overall accuracy and the SVM produced the lowest overall accuracy for highway classification. Regarding Kappa coefficient, the best accuracy was achieved by the decision tree algorithm. More importantly, the evaluation showed that the best algorithm for highway classification (based on user accuracy) is the MLP model. These evaluations were based on the sampling data. Later, these models will be evaluated regarding transferability and its performance on raster data.

5.6.3 Multilayer Perceptron

Neural networks are a set of neurons or nodes interconnected to each other by weights and output signals. In general, a neural network model consists of three layers, input, hidden, and output layers. However, several structures can be designed by modifying the number of hidden layers and the number of nodes in each hidden layer. Thus, these parameters contribute to the overall accuracy that could be achieved by the model for the classification. Here, we evaluated five different structures for the neural network to get the optimal model for road extraction from LiDAR data. These structures are one single hidden layer with three nodes, one single hidden layer with four nodes, one single hidden layer with five layers, two hidden layers with three nodes in each layer, and three hidden layers with three nodes in each layer (Fig. 5.7). The idea here is to see the effects of both some hidden layers and the number of nodes in the hidden layers. The evaluation showed that the best overall accuracy and regarding kappa coefficient could be achieved by using one single hidden layer with four nodes. However, regarding user accuracy, the best structure was found to be the three hidden layers with three nodes in each layer. This evaluation was based on the sampling data, and a second evaluation is needed to check the models for transferability issues and their applications on raster data.

Table 5.2 Proposed models for road extraction from LiDAR and digital orthophoto data

Algorithm	Proposed model	Overall accuracy (%)	Running time (s)
SVM	$-10.7086 \times$ nDSM $-8.4659 \times$ NDIR $-2.0546 \times$ Intensity $-2.0510 \times$ Color $+3.5631$ $C = 5.0$, the kernel is a polynomial function	90.19	0.02
LR	$1.1204 \times$ nDSM $+20.1763 \times$ NDIR $+0.0425 \times$ Intensity $+0.0208 \times$ Color $+9.7231$	90.38	0.09

Layout: T3_Grey Book ID: 454584_1_En Book ISBN: 978-3-030-10373-6
Chapter No.: 5 Date: 4-3-2019 Time: 2:23 pm Page: 69/75

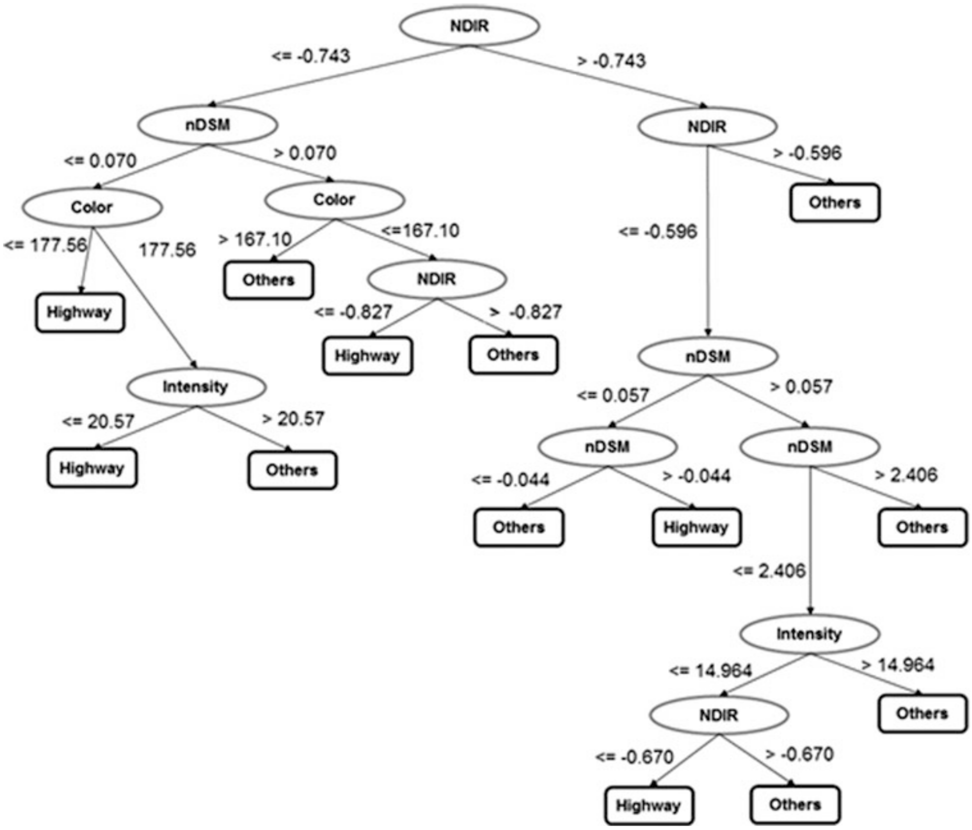

Fig. 5.5 Decision tree model proposed for highway extraction from LiDAR data

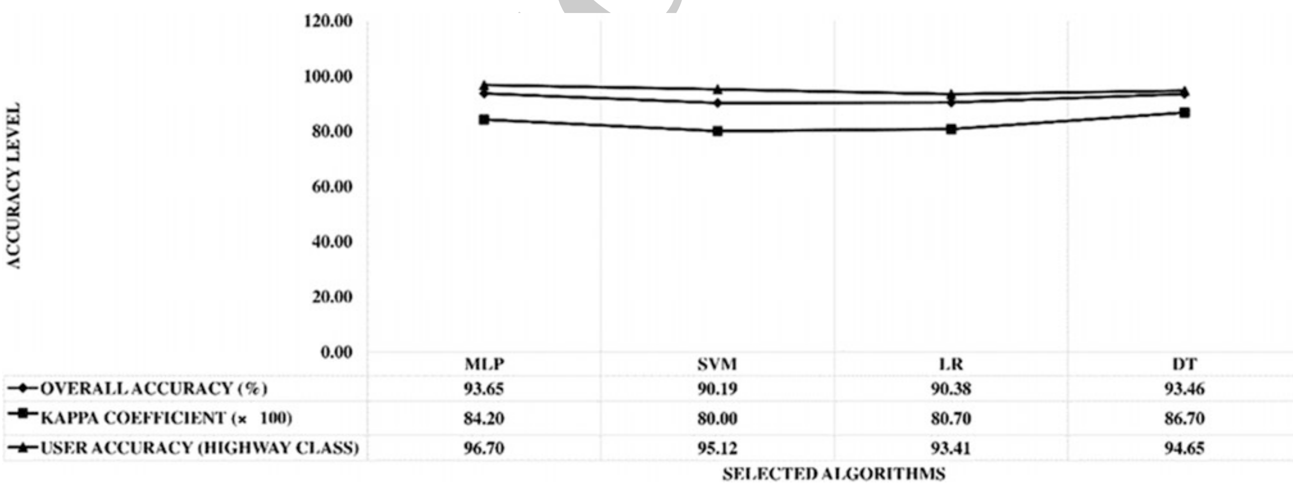

Fig. 5.6 Accuracy assessment of applied machine learning algorithms

Regarding some nodes in each hidden layer, it was noticed that the overall accuracy could improve slightly. However, unexpectedly, it was found that the number of nodes in each hidden layer did not improve the user accuracy, but the overall accuracy was decreased. In contrast, the number of hidden layers was significant for accurate highway classification in which the best user accuracy was achieved with three hidden layers.

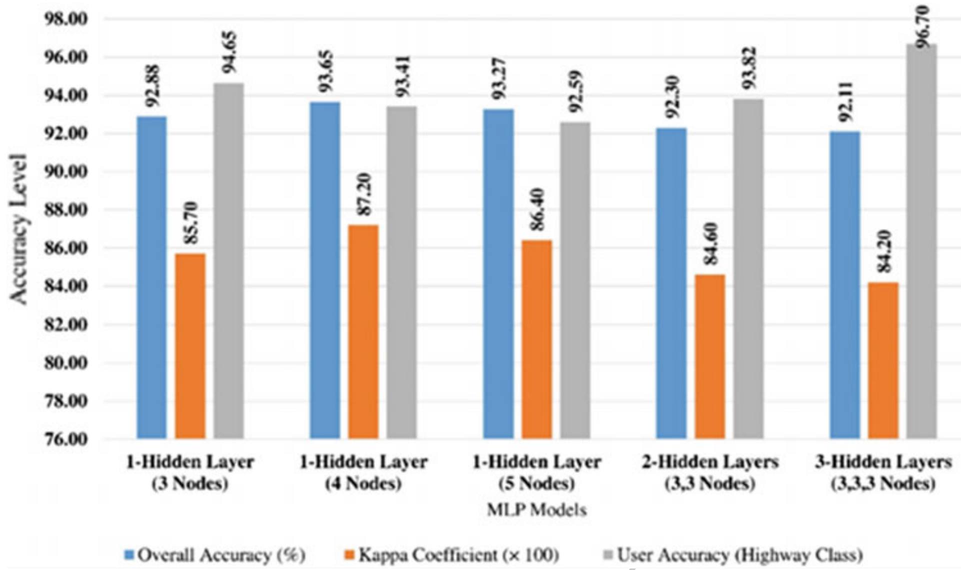

Fig. 5.7 Effects of neural network structure on the overall accuracy of highway classification

5.6.4 Support Vector Machine

It is well known that the SVM techniques are strongly dependent on the SVM hyperparameters: the regularization factor *C* and kernel function type. Thus, it was important to test several *C* parameters and kernel types and selecting the optimum parameters for highway extraction. In this study, we used trial-and-error method to evaluate each *C* and kernel function. In terms of *C* parameter, five values (0.5, 1.0, 1.5, 2.0, 3.0, and 5.0) were evaluated (Fig. 5.8). The evaluation process revealed the best *C* parameter that can accurately classify roads and non-roads is 5.0.

On the other hand, three kernel functions that could be used in SVM were evaluated for selecting the best kernel function for highway extraction from LiDAR data. These kernel functions are polynomial, radial basis function (RBF), and Pearson VII universal kernel (PUK). The evaluation revealed that the highest overall accuracy could be achieved with PUK kernel, while the RBF kernel is the best for highway extraction based on user accuracy measure. The details of kernel function evaluation on SVM classifier for highway extraction are shown in Fig. 5.9.

5.6.5 Applications on Raster Data and Models Transferability Issues

One of the difficult and challenging tasks in model development is to make it general, which could be applied to different datasets. Here, we aim to test the developed ML models on raster data and investigate their transferability. As mentioned above, the overall accuracy achieved by the proposed models is 93.65, 90.19, 90.38, and 93.46% for MLP, SVM, LR, and DT, respectively. By applying the complete GIS workflow, we achieved the following overall road extraction results (Fig. 5.10). Both visual and

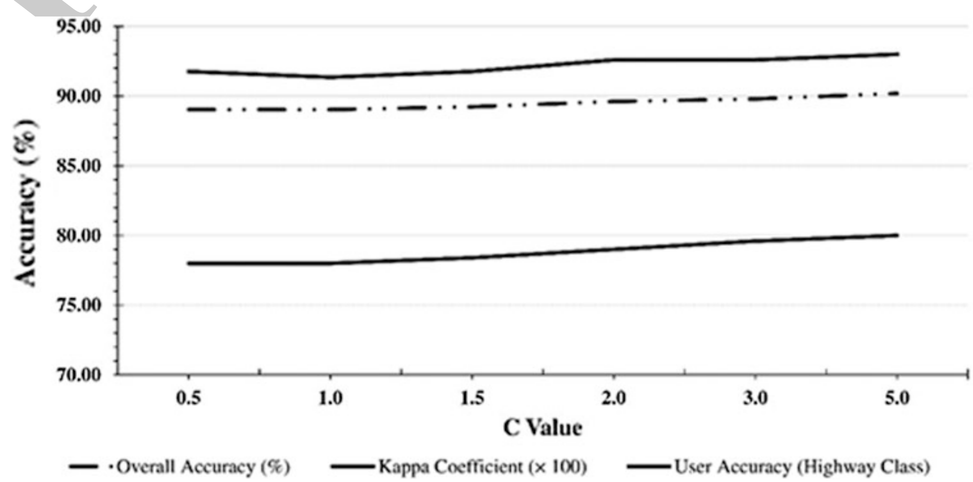

Fig. 5.8 Effects of *C* value on SVM classifier

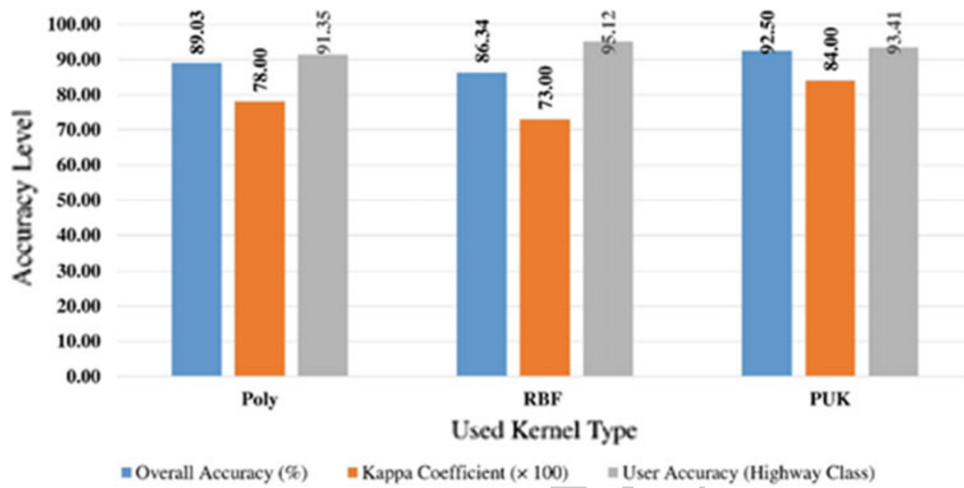

Fig. 5.9 Effects of kernel function types on SVM classifier

quantitative interpretation show that the logistic regression model has produced the highest quality road extraction (Fig. 5.10f). In this result, one can notice that the most of the road features were classified accurately and correctly. One problem occurred in this model is that the elevated roads were not detected as well as the height attribute is higher than the normal values (around 0). The result from DT model was also sophisticated in which most of the road feature extracted correctly and the elevated roads to some extent was detected (Fig. 5.10h). However, there were some random noises and some of the road features within built-up areas not detected totally as in the left down of Fig. 5.10h. The MLP model detected the elevated roads correctly, while there were some misclassifications features, which produced random noises in the result (Fig. 5.10b). In addition, the boundary of road features was not detected accurately when the MLP model was used. Although SVM model could classify roads and non-roads with high overall accuracy (90.19%) when using sampling data, the application of SVM model on raster data has produced very low-quality result (Fig. 5.10d). From this result, it can be inferred that SVM model suffers from transferability issues and needs for further research to optimize it for road extraction from LiDAR data.

5.6.6 Quantitative Evaluation of Road Extraction

The accuracy assessment of road extraction is usually performed using three evaluation measures introduced by Wiedemann et al. (1998), the completeness, correctness, and quality.

Completeness measure: The completeness is defined as the ratio of the true positives from the sum of the true positives and false negatives given by,

$$\text{Completeness} = \frac{\text{TP}}{\text{TP} + \text{FN}} \tag{5.9}$$

Correctness measure: The correctness is defined as the ratio of the true positives from the sum of the true and false positives given by,

$$\text{Correctness} = \frac{\text{TP}}{\text{TP} + \text{FP}} \tag{5.10}$$

Quality measure: The quality is a measure of the 'goodness' of the final result and is given by,

$$\text{Quality} = \frac{\text{TP}}{\text{TP} + \text{FP} + \text{FN}} \tag{5.11}$$

where TP, TN, FP, and FN stand for true positives, true negatives, false positives, and false negatives, respectively.

Keeping in mind that the optimal values for the three measures are 1, 100% of completeness means that all roads are recovered, 100% of correctness means that all roads extracted are actual roads and 100% of quality means that all roads are correct and complete. The evaluation strategy is presented in Fig. 5.11c, which shows the true positives, false positives, and false negatives parameters.

Table 5.3 shows the evaluation measures for the four proposed models. These evaluations were done based on the ground reference data (Fig. 5.11a) derived from the aerial photograph by manual digitizing. As it is evident from the results and the accuracy measures presented in Table 5.3, the proposed simple integrated GIS model performs well when

Layout: T3_Grey Book ID: 454584_1_En Book ISBN: 978-3-030-10373-6
Chapter No.: 5 Date: 4-3-2019 Time: 2:23 pm Page: 72/75

Fig. 5.10 Results of highway extraction models, **a** MLP, **b** filtered MLP, **c** SVM, **d** filtered SVM, **e** LR, **f** filtered LR, **g** DT, **h** filtered DT

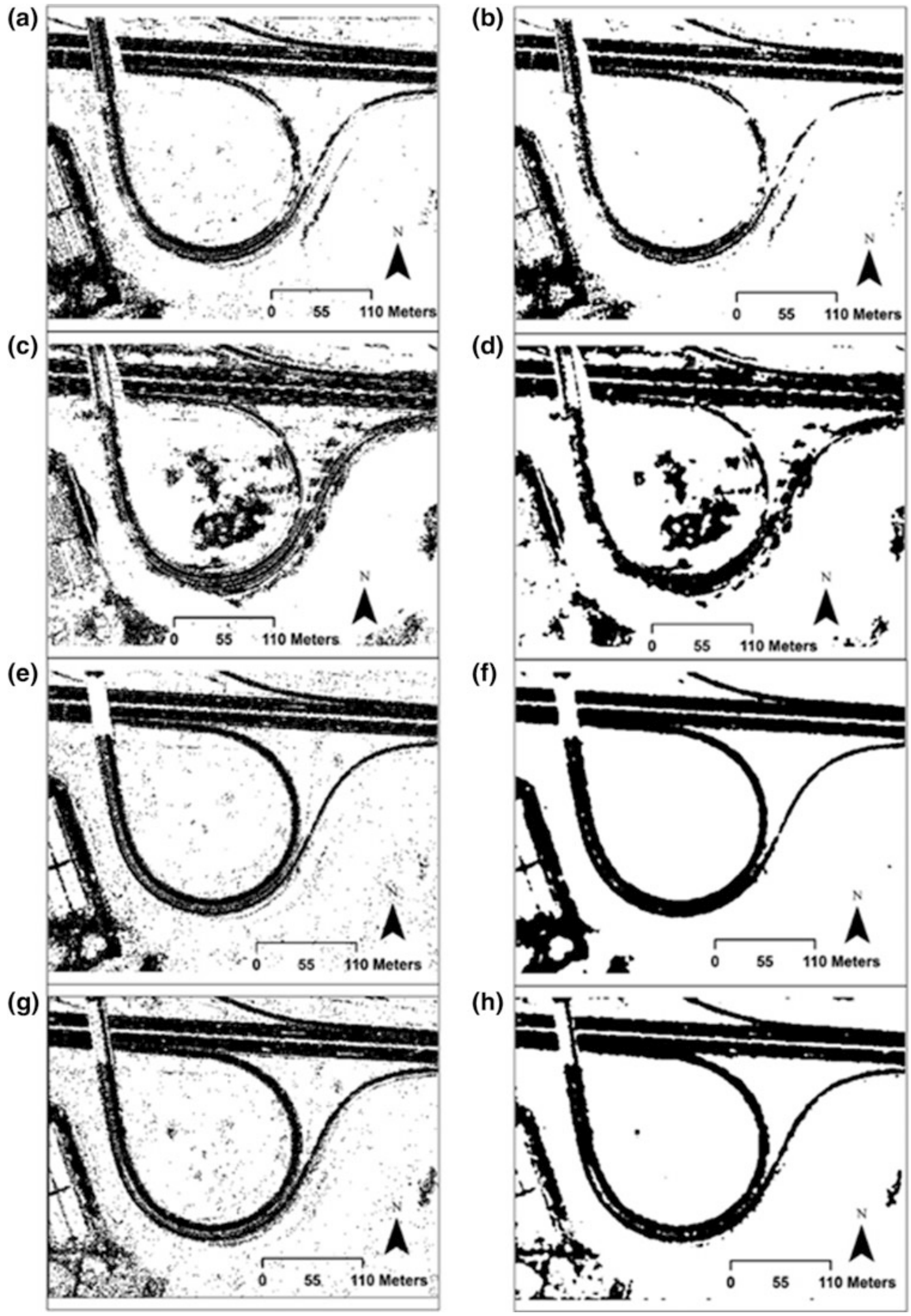

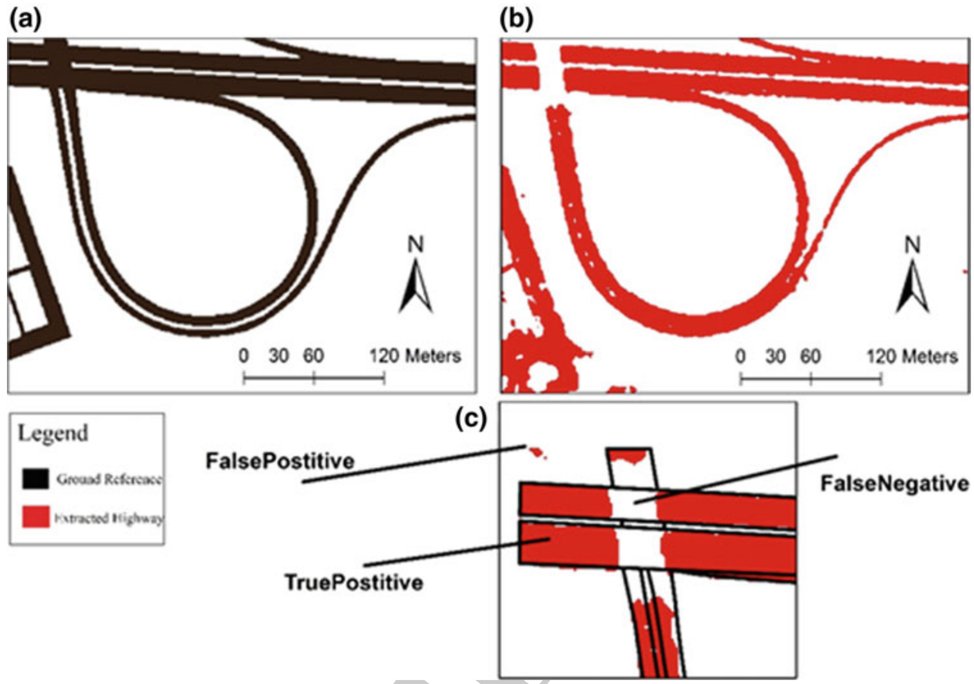

Fig. 5.11 Ground reference data and highway extraction evaluation strategy, **a** ground reference data generated by manual digitizing of an aerial photograph, **b** extracted highway using logistic regression model, **c** evaluation strategy of highway extraction

Table 5.3 Proposed models for road extraction from LiDAR and digital orthophoto data

Models	Evaluation measures		
	Completeness (%)	Correctness (%)	Quality (%)
MLP	78.34	69.72	58.45
SVM	61.09	50.81	38.38
LR	85.43	76.70	67.82
DT	81.12	73.05	62.43

using either logistic regression or decision tree model in highway detection module. The success of our approach depends primarily on machine learning approach, which optimizes the feature extraction from a set of input variables.

5.7 Conclusion

In this paper, several machine learning algorithms were evaluated namely multilayer perceptron, support vector machine, logistic regression, and decision tree for automatic and reliable highway detection from airborne LiDAR data and aerial photographs. Then, a simple integrated GIS workflow was proposed for automatic extraction of highways using the optimum machine learning model determined from the evaluation study. The GIS workflow proposed in this study is an integrated model which merges the strengths of data preprocessing, highway detection based on machine learning, and post-processing (majority filtering). The proposed workflow together with the developed machine learning models has addressed the challenges of automatic detection and extraction of highways from airborne LiDAR data.

Firstly, this study investigated the effects of the RGB format of the aerial photograph on the highway detection, and it was found that the transformation into L-a-b color space system is critical to reducing the illumination effects. Four raster datasets (such as height, NDIR, intensity, and color datasets) were derived from the original LiDAR data and aerial photograph to be inputs for the model's development. Using randomly selected 1700 points from the aerial orthophoto, four machine learning-based models were developed. The developed models were then applied on a raster dataset to detect the highways and separate them from other objects. The result of the detected highway was refined by applying a majority spatial filter producing the final product that could be used for various geospatial applications.

Second, the evaluation study revealed that logistic regression is the best model to be used with an overall accuracy of (90.38%) on sampling data. When the model was applied to raster data, the result showed that this model is reliable and provided highly accurate road extraction from LiDAR data. The logistic regression model achieved the accuracy of 85.43, 76.70, and 62.43% for completeness, correctness, and quality. However, logistic regression model could not detect elevated roads well whereas neural network did. For that reason, the future research direction for automatic road extraction is to use ensemble methods. Ensemble methods can combine multiclassier to get the advantages of both classifiers. This will ensure high-quality road extraction as well as to elevated roads problem can be solved.

The evaluation test has shown that the proposed GIS workflow performs well for automatic highway extraction in a simple GIS-based method. In addition, the developed GIS model can be implemented in most commercial and open-source GIS software, which makes it powerful, and efficient for industrial use.

References

Alharthy, A., & Bethel, J. (2003). Automated road extraction from LIDAR data. In *Proceedings of the ASPRS Annual Conference, 2003* (pp. 05–09).

Amo, M., Martínez, F., & Torre, M. (2006). Road extraction from aerial images using a region competition algorithm. *IEEE Transactions on Image Processing, 15,* 1192–1201.

Antonarakis, A. S., Richards, K. S., & Brasington, J. (2008). Object-based land cover classification using airborne LiDAR. *Remote Sensing of Environment, 112,* 2988–2998.

Baczyński, D., & Parol, M. (2004). Influence of artificial neural network structure on quality of short-term electric energy consumption forecast. *IEE Proceedings-Generation, Transmission and Distribution, 151,* 241–245.

Bazi, Y., & Melgani, F. (2006). Toward an optimal SVM classification system for hyperspectral remote sensing images. *IEEE Transactions on Geoscience and Remote Sensing, 44,* 3374–3385.

Bentaleb, K., Lakouari, N., Marzoug, R., Ez-Zahraouy, H., & Benyoussef, A. (2014). Simulation study of traffic car accidents in single-lane highway. *Physica A: Statistical Mechanics and its Applications, 413,* 473–480.

Boyko, A., & Funkhouser, T. (2011). Extracting roads from dense point clouds in large scale urban environment. *ISPRS Journal of Photogrammetry and Remote Sensing, 66,* S2–S12.

Brennan, R., & Webster, T. (2006). Object-oriented land cover classification of lidar-derived surfaces. *Canadian Journal of Remote Sensing, 32,* 162–172.

Briese, C., Pfeifer, N., & Dorninger, P. (2002). Applications of the robust interpolation for DTM determination. *International Archives of Photogrammetry Remote Sensing and Spatial Information Sciences, 34,* 55–61.

Butenuth, M., Straub, B.-M., Heipke, C., & Willrich, F. (2003). Tree supported road extraction from arial images using global and local context knowledge. In *Computer vision systems* (pp. 162–171). Berlin: Springer.

Choi, Y.-W., Jang, Y.-W., Lee, H.-J., & Cho, G.-S. (2008). Three-dimensional LiDAR data classifying to extract road point in urban area. *IEEE Geoscience and Remote Sensing Letters, 5,* 725–729.

Clode, S., Kootsookos, P. J., & Rottensteiner, F. (2004). The automatic extraction of roads from LIDAR data. ISPRS 2004.

Coren, F., & Sterzai, P. (2006). Radiometric correction in laser scanning. *International Journal of Remote Sensing, 27,* 3097–3104.

Ding, S., Xu, X., & Nie, R. (2013). Extreme learning machine and its applications. *Neural Computing and Applications, 25,* 549–556.

Evans, J. S., & Hudak, A. T. (2007). A multiscale curvature algorithm for classifying discrete return lidar in forested environments. *IEEE Transactions on Geoscience and Remote Sensing, 45,* 1029–1038.

Friedl, M. A., & Brodley, C. E. (1997). Decision tree classification of land cover from remotely sensed data. *Remote Sensing of Environment, 61,* 399–409.

Gardner, M. W., & Dorling, S. R. (1998). Artificial neural networks (the multilayer perceptron)—A review of applications in the atmospheric sciences. *Atmospheric Environment, 32,* 2627–2636.

Gokgoz, E., & Subasi, A. (2015). Comparison of decision tree algorithms for EMG signal classification using DWT. *Biomedical Signal Processing and Control, 18,* 138–144.

Gong, L., Zhang, Y., Li, Z., & Bao, Q. (2010). Automated road extraction from LiDAR data based on intensity and aerial photo. In *2010 3rd International Congress on Image and Signal Processing (CISP)* (pp. 2130–2133).

Hodgson, M. E., Jensen, J. R., & Im, J. (2008). Object-based land cover classification using high-posting-density LiDAR Data. *GIScience & Remote Sensing, 45,* 209–228.

Hu, X., Tao, C. V., & Hu, Y. (2004). Automatic road extraction from dense urban area by integrated processing of high resolution imagery and lidar data. In *International archives of photogrammetry, remote sensing and spatial information sciences*. Istanbul, Turkey (Vol. 35, p. B3).

Hu, X., Li, Y., Shan, J., Zhang, J., & Zhang, Y. (2014). Road centerline extraction in complex urban scenes from LiDAR data based on multiple features. *IEEE Transactions on Geoscience and Remote Sensing, 52,* 7448–7456.

Jebur, M. N., Pradhan, B., & Tehrany, M. S. (2014). Optimization of landslide conditioning factors using very high-resolution airborne laser scanning (LiDAR) data at catchment scale. *Remote Sensing of Environment, 152,* 150–165.

Kim, J. G., Han, D. Y., Yu, K. Y., Kim, Y. I., & Rhee, S. M. (2006). Efficient extraction of road information for car navigation applications using road pavement markings obtained from aerial images. *Canadian Journal of Civil Engineering, 33,* 1320–1331.

Lary, D. J., Alavi, A. H., Gandomi, A. H., & Walker, A. L. (2015). Machine learning in geosciences and remote sensing. *Geoscience Frontiers*.

Li, J., Lee, H. J., & Cho, G. S. (2008). Parallel algorithm for road points extraction from massive LiDAR data (pp. 308–315).

Mašetic, Z., & Subasi, A. (2013). Detection of congestive heart failures using C4. 5 Decision Tree.

Matkan, A. A., Hajeb, M., & Sadeghian, S. (2014). Road extraction from lidar data using support vector machine classification. *Photogrammetric Engineering & Remote Sensing, 80,* 409–422.

Melgani, F., & Bruzzone, L. (2004). Classification of hyperspectral remote sensing images with support vector machines. *IEEE Transactions on Geoscience and Remote Sensing, 42,* 1778–1790.

Mena, J. B., & Malpica, J. A. (2005). An automatic method for road extraction in rural and semi-urban areas starting from high resolution satellite imagery. *Pattern Recognition Letters, 26,* 1201–1220.

Mia, M. M. A., Biswas, S. K., Urmi, M. C., & Siddique, A. (2015). An algorithm for training multilayer perceptron (MLP) for image reconstruction using neural network without overfitting.

Mokhtarzade, M., & Zoej, M. J. V. (2007). Road detection from high-resolution satellite images using artificial neural networks. *International Journal of Applied Earth Observation and Geoinformation, 9,* 32–40.

Mountrakis, G., Im, J., & Ogole, C. (2011). Support vector machines in remote sensing: A review. *ISPRS Journal of Photogrammetry and Remote Sensing, 66,* 247–259.

Nandi, A., & Shakoor, A. (2010). A GIS-based landslide susceptibility evaluation using bivariate and multivariate statistical analyses. *Engineering Geology, 110,* 11–20.

Oommen, T., Misra, D., Twarakavi, N. K. C., Prakash, A., Sahoo, B., & Bandopadhyay, S. (2008). An objective analysis of support vector machine based classification for remote sensing. *Mathematical Geosciences, 40,* 409–424.

Peng, T., Jermyn, I. H., Prinet, V., & Zerubia, J. (2010). Extended phase field higher-order active contour models for networks. *International Journal of Computer Vision, 88,* 111–128.

Platt, J. C. (1999). Using analytic QP and sparseness to speed training of support vector machines. In *Advances in neural information processing systems* (pp. 557–563).

Poullis, C., & You, S. (2010). Delineation and geometric modeling of road networks. *ISPRS Journal of Photogrammetry and Remote Sensing, 65,* 165–181.

Priddy, K. L., & Keller, P. E. (2005). Artificial neural networks: an introduction (Vol. 68). SPIE Press.

Quinlan, J. R. (2014). C4. 5: Programs for machine learning. Elsevier.

Rottensteiner, F. (2009). Status and further prospects of object extraction from image and laser data. In *2009 Joint Urban Remote Sensing Event* (pp. 1–10).

Rottensteiner, F. (2010). Automation of object extraction from LiDAR in urban areas. In *2010 IEEE International Geoscience and Remote Sensing Symposium (IGARSS)* (pp. 1343–1346).

Saghebian, S. M., Sattari, M. T., Mirabbasi, R., & Pal, M. (2013). Ground water quality classification by decision tree method in Ardebil region, Iran. *Arabian Journal of Geosciences, 7,* 4767–4777.

Samadzadegan, F., & Bigdeli, B. (2009). Combining multiple classifiers for automatic road extraction from lidar data.

Soliman, O. S. & Mahmoud, A. S. (2012). A classification system for remote sensing satellite images using support vector machine with non-linear kernel functions. In *2012 8th International Conference on Informatics and Systems (INFOS)* (pp. BIO-181–BIO-187).

Song, M., & Civco, D. (2004). Road extraction using SVM and image segmentation. *Photogrammetric Engineering & Remote Sensing, 70,* 1365–1371.

Vaa, T., Penttinen, M., & Spyropoulou, I. (2007). Intelligent transport systems and effects on road traffic accidents: State of the art. *IET Intelligent Transport Systems, 1,* 81.

Vapnik, V. (2013). The nature of statistical learning theory. Berlin: Springer.

Wan, Y., Shen, S., Song, Y., & Liu, S. (2007). A road extraction approach based on fuzzy logic for high-resolution multispectral data. In *Fourth International Conference on Fuzzy Systems and Knowledge Discovery, 2007 (FSKD 2007)* (pp. 203–207).

Wang, G., Zhang, Y., Li, J., & Song, P. (2011). 3D road information extraction from LIDAR data fused with aerial-images. In *2011 IEEE International Conference on Spatial Data Mining and Geographical Knowledge Services (ICSDM)* (pp. 362–366).

White, R. A., Dietterick, B. C., Mastin, T., & Strohman, R. (2010). Forest roads mapped using LiDAR in steep forested terrain. *Remote Sensing, 2,* 1120–1141.

Wiedemann, C., Heipke, C., Mayer, H., & Hinz, S. (1998). Automatic extraction and evaluation of road networks from MOMS-2P imagery. *International Archives of Photogrammetry and Remote Sensing, 32,* 285–291.

Yang, G. Y. C. (1995). Geological mapping from multi-source data using neural networks: Geomatics engineering. University of Calgary.

Yao, W., & Han, M. (2011). Remote sensing image classification with parameter optimized support vector machine based on evolutionary computation. In *2011 Fourth International Workshop on Advanced Computational Intelligence (IWACI)* (pp. 290–294).

Zhan, Y., & Shen, D. (2005). Design efficient support vector machine for fast classification. *Pattern Recognition, 38,* 157–161.

Zhao, J., & You, S. (2012). Road network extraction from airborne LiDAR data using scene context. In *2012 IEEE Computer Society Conference on Computer Vision and Pattern Recognition Workshops (CVPRW)* (pp. 9–16).

Zhao, Y., & Zhang, Y. (2008). Comparison of decision tree methods for finding active objects. *Advances in Space Research, 41,* 1955–1959.

Zhao, J., You, S., & Huang, J. (2011). Rapid extraction and updating of road network from airborne LiDAR data. In *2011 IEEE Applied Imagery Pattern Recognition Workshop (AIPR)* (pp. 1–7). AQ5

Zhou, W. (2013). An object-based approach for urban land cover classification: Integrating LiDAR height and intensity data. *IEEE Geoscience and Remote Sensing Letters, 10,* 928–931.

Zhu, P., Lu, Z., Chen, X., Honda, K., & Eiumnoh, A. (2004). Extraction of city roads through shadow path reconstruction using laser data. *Photogrammetric Engineering & Remote Sensing, 70,* 1433–1440.

Zhu, H., Yang, X., & Luo, Y. (2009). Classification of urban remote sensing image based on support vector machines. In *2009 17th International Conference on Geoinformatics* (pp. 1–6).